Article

Cell

Oncogenic Role of Fusion-circRNAs Derived from Cancer-Associated Chromosomal Translocations

Graphical Abstract

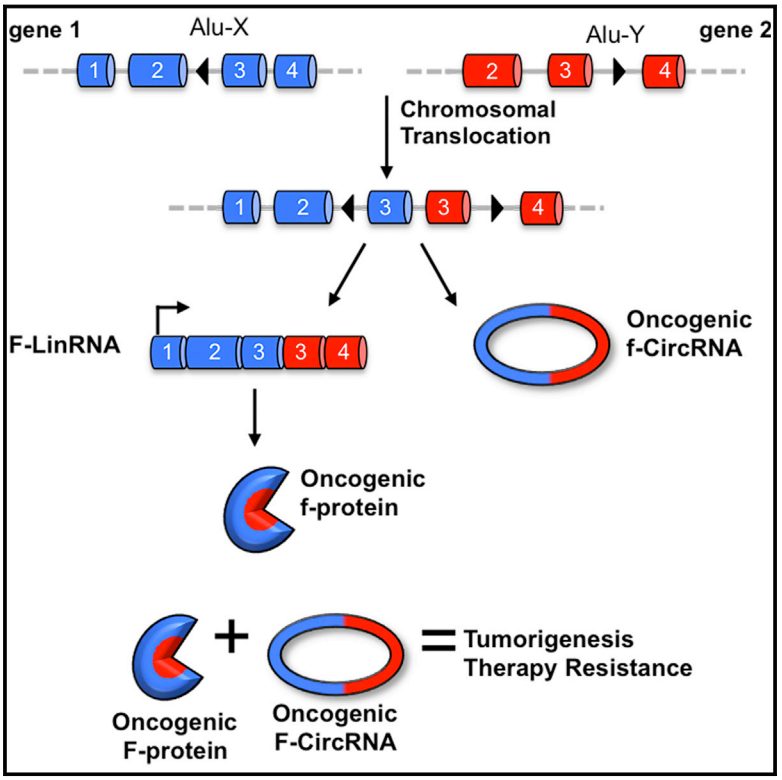

Authors

Jlenia Guarnerio, Marco Bezzi, Jong Cheol Jeong, ..., Yvonne Tay, Andrew H. Beck, Pier Paolo Pandolfi

Correspondence

ppandolf@bidmc.harvard.edu

In Brief

Chromosomal translocations associated with cancer give rise to fusion circRNAs which contribute to cellular transformation, affect cell viability, and have tumor-promoting properties in in vivo models.

Highlights

- F-circRNAs are generated from cancer-associated chromosomal translocations
- F-circRNAs promote transformation and cell survival upon treatment
- F-circRNAs confer resistance to treatment in tumor cells

Accession Numbers

EF406122
AB067754

Guarnerio et al., 2016, Cell *165*, 289–302
April 7, 2016
http://dx.doi.org/10.1016/j.cell.2016.03.020

CellPress

Cell

Oncogenic Role of Fusion-circRNAs Derived from Cancer-Associated Chromosomal Translocations

Jlenia Guarnerio,[1] Marco Bezzi,[1] Jong Cheol Jeong,[2] Stella V. Paffenholz,[1] Kelsey Berry,[1] Matteo M. Naldini,[1] Francesco Lo-Coco,[3] Yvonne Tay,[4] Andrew H. Beck,[2] and Pier Paolo Pandolfi[1,*]

[1]Cancer Research Institute, Beth Israel Deaconess Cancer Center, Departments of Medicine and Pathology, Beth Israel Deaconess Medical Center, Harvard Medical School, Boston, MA 02215, USA

[2]Cancer Research Institute, Beth Israel Deaconess Cancer Center, Department of Pathology, Beth Israel Deaconess Medical Center, Harvard Medical School, Boston, MA 02215, USA

[3]Department of Biomedicine and Prevention, University Tor Vergata, and Fondazione Santa Lucia, 00173 Rome, Italy

[4]Cancer Science Institute of Singapore and Department of Biochemistry, Yong Loo Lin School of Medicine, National University of Singapore, Singapore 117597, Singapore

*Correspondence: ppandolf@bidmc.harvard.edu

http://dx.doi.org/10.1016/j.cell.2016.03.020

SUMMARY

Chromosomal translocations encode oncogenic fusion proteins that have been proven to be causally involved in tumorigenesis. Our understanding of whether such genomic alterations also affect non-coding RNAs is limited, and their impact on circular RNAs (circRNAs) has not been explored. Here, we show that well-established cancer-associated chromosomal translocations give rise to fusion circRNAs (f-circRNA) that are produced from transcribed exons of distinct genes affected by the translocations. F-circRNAs contribute to cellular transformation, promote cell viability and resistance upon therapy, and have tumor-promoting properties in in vivo models. Our work expands the current knowledge regarding molecular mechanisms involved in cancer onset and progression, with potential diagnostic and therapeutic implications.

INTRODUCTION

Recurrent genomic alterations such as point mutations, chromosomal deletions, amplifications, and translocations have been historically associated with the pathogenesis of several diseases, including cancer (Chin et al., 2011; Meyerson et al., 2010; Rabbitts, 1994). The role of genomic alterations in the process of tumorigenesis is attributed to their capacity to affect or generate proto-oncogenic and tumor suppressive proteins. Such proteins are generally mutated versions of functional cellular proteins and are often the primary cause of the onset and progression of cancer. For instance, cancer-associated aberrant chromosomal translocations that result in the rearrangement of parts of non-homologous chromosomes can join together two otherwise-separated genes leading to the formation of a "fusion gene." As a result, a downstream gene may fall under the promoter of the upstream gene and, in some instances, in the transcription of a fusion mRNA that is often, but not always, translated into a protein made from elements of both genes. Such proteins are labeled as oncogenic "fusion proteins" (Greuber et al., 2013; Somervaille and Cleary, 2010).

Although oncogenic proteins are undoubtedly critical factors in cancer development, there is mounting evidence demonstrating that proteins are not the only entities involved in disease pathogenesis. The non-coding dimension, which includes microRNAs (miRNAs) (Croce, 2009; Ryan et al., 2010), pseudogenes (Karreth et al., 2015), long-non-coding RNAs (lncRNAs) (Cheetham et al., 2013), and the recently re-discovered circular RNAs (circRNAs) (Jeck et al., 2013; Li et al., 2015a; Qu et al., 2015), is drawing renewed attention in cancer research. However, whether and how genomic alterations impact the non-coding RNA dimension has been, so far, only poorly investigated (Calin and Croce, 2007), and their impact on circRNAs is completely unexplored.

Discovered more than 30 years ago (Hsu and Coca-Prados, 1979), circRNAs have not been a focal point of research until recently, when new reports began to show their direct involvement in multiple biological processes (Jeck and Sharpless, 2014; Jeck et al., 2013; Qu et al., 2015; Hansen et al., 2013; Memczak et al., 2013). Additionally, several recent publications have convincingly demonstrated that the formation of circRNAs is not just a result of splicing errors. The biogenesis of circRNAs is instead actively regulated and favored by the presence of specific and repetitive sequences' and RNA-binding proteins' (RBPs) binding sites within the introns up- and downstream of the circularizing exons (Ashwal-Fluss et al., 2014; Barrett et al., 2015; Conn et al., 2015; Jeck et al., 2013; Liang and Wilusz, 2014; Zhang et al., 2014). Thus, circRNAs are described as the result of a proactive back-splice event, in which the 3′ tail of one exon is joined to the 5′ head of an upstream exon (Jeck et al., 2013). Although some of the molecular and biological roles played by circRNAs have been characterized (Hansen et al., 2013; Li et al., 2015d; Memczak et al., 2013; You et al., 2015), the function of circRNAs remains largely unknown.

Multiple tumor types including liquid and solid tumors are associated with recurrent chromosomal translocations (Rabbitts,

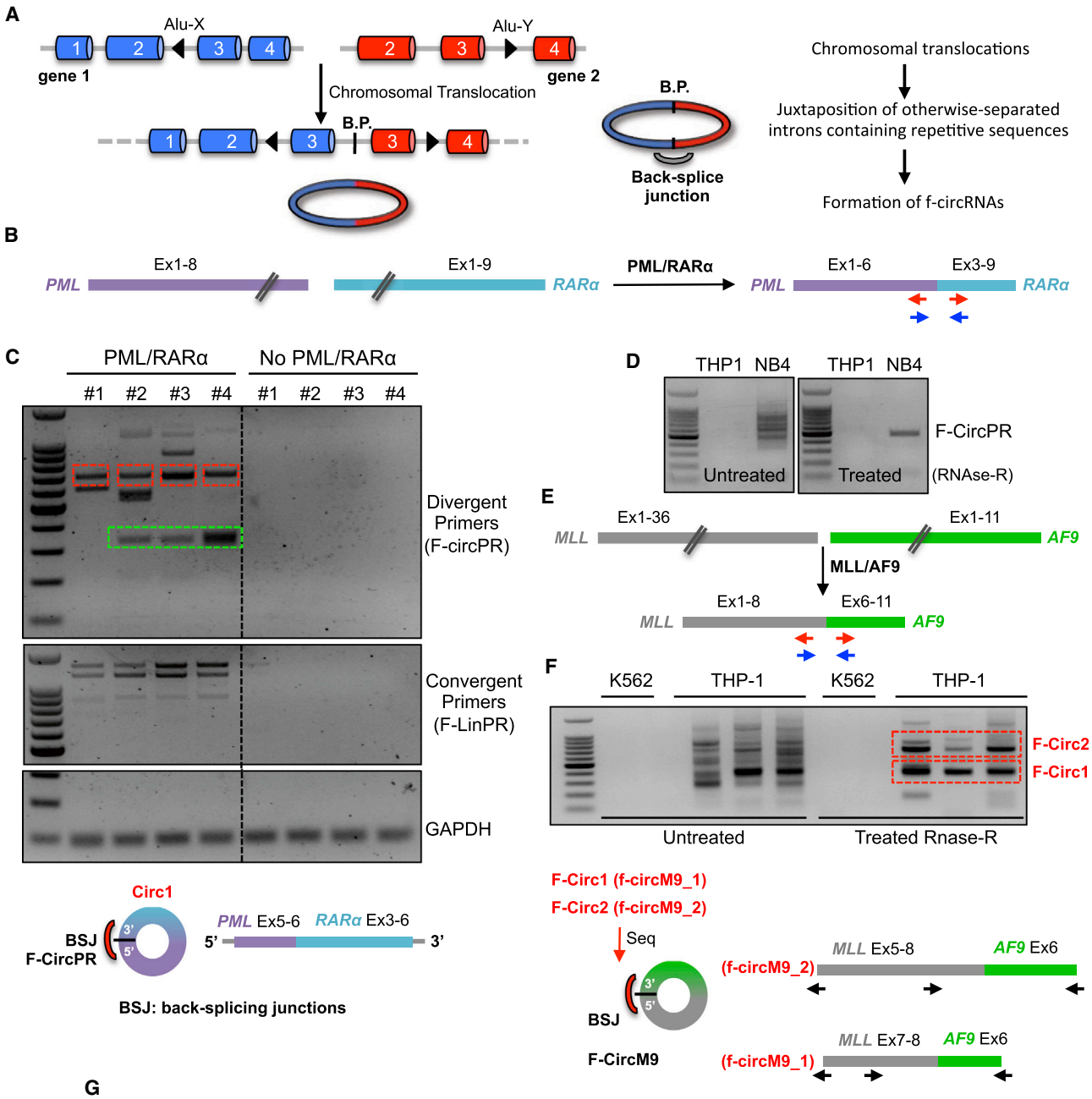

G

Parameters MA=MLL/AF9 PR=PML/RARα					Method 1					
					Circular		Linear			
					MA	PR	MA		PR	
Samples	Fusion	*n*	*l*	*w*	*Gen*	*Gen*	*Exp*	*Gen*	*Exp*	*Gen*
THP1	MLL/AF9	1	42	35	1	0	4	0	0	0
THP1	MLL/AF9	1	20	10	7	0	2	1	0	0
NB4	PML/RARα	1	40	30	0	0	0	0	0	0
NB4	PML/RARα	2	40	35	1	0	0	0	2	0
NB4	PML/RARα	2	42	35	0	2	0	0	0	6
APL_1	PML/RARα	1	42	35	0	0	0	0	0	0
APL_2	PML/RARα	1	48	30	0	1	0	0	0	5
APL_3	PML/RARα	2	43	35	0	1	0	0	0	1
APL_4	PML/RARα	1	43	35	0	1	0	0	0	3
CTR		2	44	35	0	0	0	0	0	0

(legend on next page)

1994; Bunting and Nussenzweig, 2013). Here, we show that tumors harboring chromosomal translocations also harbor circRNAs derived from the rearranged genome: aberrant fusion-circRNAs (f-circRNA). We further show that such f-circRNAs can be functionally relevant and tumor promoting, with potential diagnostic and therapeutic implications.

RESULTS

F-circRNAs Are a Product of Aberrant Chromosomal Translocations in Cancer Cells

Multiple tumor types are characterized by the presence of aberrant chromosomal translocations and chromosomal rearrangements (Rabbitts, 1994; Bunting and Nussenzweig, 2013). These rearrangements result first in the juxtaposition of two otherwise-separated genes, then in the transcription of a fused mature mRNA, and finally in the expression of specific fusion oncogenic proteins (Rabbitts, 1994). Because genes are incorrectly reallocated, we hypothesized that distant, unrelated intronic sequences of the translocated genes may also be juxtaposed. As a consequence, complementary repetitive intronic sequences (e.g., Alu-sequences) could be brought in at a close enough proximity to favor new events of back-splicing during the process or RNA maturation, which would result in the generation of aberrant circRNAs (Barrett et al., 2015; Jeck et al., 2013; Liang and Wilusz, 2014; Zhang et al., 2014). We thus hypothesized that the juxtaposition of complementary sequences in introns up- and downstream of the breakpoint region of the translocation could allow the formation of new circRNAs, f-circRNAs, made by the fusion of the two translocated genes (Figure 1A). In order to investigate this possibility, we at first used primers diverging from the breakpoint of the translocation and we looked for the presence of f-circRNAs through PCR assays.

Several types of leukemia are known to carry distinctive chromosomal translocations, among them, *PML/RARα* is the most recurrent translocation in patients with acute promyelocytic leukemia (APL) (Dos Santos et al., 2013). In this translocation, the main break point cluster region (BCR) of the *PML* gene is located in intron 6, while the main BCR of *RARα*, the partner gene of PML, lays in intron 2 (Figure 1B) (Dekking et al., 2012). Using primary samples from patients that harbor this translocation, we investigated whether *PML/RARα* could generate f-circRNAs (f-circPR for brevity). Total RNA was extracted from bone marrow (BM)-derived leukemic cells of APL patients, or human primary leukemic cells of control, and subjected to treatment with RNase-R (Jeck and Sharpless, 2014). Divergent primers were next used to amplify possible f-circPRs (Figures 1B and S1A). All of the analyzed patients that carry the *PML/RARα* translocation (confirmed by the use of convergent primers spanning the break point; Figures 1B and 1C) displayed the expression of one or more f-circPR (Figure 1C). By sequencing the PCR products, we ascertained that all of the patients expressed an isoform of f-circPR with the back-splice junction between the 5′ head of *PML* exon 5 and the 3′ tail of *RARα* exon 6 (Figure S1B). However, three out of four patients showed expression of an additional, alternative f-circPR, whose back-splice junction occurs between the exon 4 of *PML* and the exon 4 of *RARα* (Figures 1C and S1B). In order to further validate these results, we also analyzed the presence of f-circRNA in the APL-derived leukemic cell line NB4 (Lanotte et al., 1991). Only one f-circRNA was detected in the NB4 cells, whose back-splice junction was sequenced between the 5′ head of the exon 5 of *PML* and the 3′ tail of the exon 6 of *RARα* (Figures 1D and S1C). We concluded that, as a result of a paradigmatic chromosomal translocation such as the t(15;17) of APL, the *PML/RARα* fusion gene can give rise to one or more f-circRNAs.

We next extended our investigation of f-circRNAs to other chromosomal translocations. The *MLL* gene has multiple fusion partners in acute myeloid leukemia (Krivtsov and Armstrong, 2007), and among them, a recurrent fusion partner is *AF9* (*MLLT3*). We thus investigated whether the *MLL/AF9* aberrant translocation could also generate f-circRNAs. To this end, we used THP1 cells in which *MLL* is broken after exon 8 and is joined to *AF9*, which loses its first 5 exons (Tsuchiya et al., 1980) (Figures 1E and S1D). Amplification with primers diverging from the breakpoint followed by Sanger sequence revealed that *MLL/AF9* translocation bears two distinct f-circRNAs (f-circM9_1 and f-circM9_2 for brevity). f-circM9_1 displayed its back-splice junction between the 5′ head of *MLL* exon 7 and the 3′ tail of *AF9* exon 6, while f-circM9_2 displayed its back-splice junction between the 5′ head of *MLL* exon 5 and the 3′ tail of *AF9* exon 6 (Figures 1F and S1E). Thus, multiple f-circRNAs can be generated from *PML-RARα* and *MLL/AF9* fusion genes.

Finally, we investigated whether the formation of f-circRNAs is an exclusive feature of leukemic cells, or whether it is also common to tumors of different histological origins. To this end, we analyzed solid tumors, and investigated if the *EWSR1/FLI1* translocation, associated with Ewing Sarcoma (Anderson et al., 2012), and the *EML4/ALK1* translocation, associated with lung cancer (Martelli et al., 2009), could also originate from f-circRNAs. SK-NEP-1 sarcoma cell line cells (Smith et al., 2008) and H3122 lung cancer cell lines were therefore used for

Figure 1. F-circRNAs Derive from Cancer-Associated Chromosomal Translocations

(A) Schematic representation of the working hypothesis (BP, breakpoint).

(B) Schematic representation of the *PML/RARα* translocation that occurs in APL.

(C) PCR analysis of RNAs derived from primary leukemic cells harboring *PML/RARα* translocation or different translocations (controls). Divergent primers are used to detect f-circRNAs and convergent primers are used to detect the breakpoint of the translocation. Bands highlighted have been Sanger-sequenced and ascertained as f-circRNAs. The results are schematically represented in the lower part of the panel.

(D) PCR analysis of the RNA derived from NB4 or THP1 cells for the identification of f-circPR. Divergent primers were used.

(E) Schematic representation of the *MLL/AF9* translocation found in THP1 cell line.

(F) PCR analysis of RNAs derived from THP1 and K562 cells. Divergent primers were used to detect f-circM9. Bands highlighted were Sanger-sequenced, and the results are schematically represented in the lower part of the panel.

(G) Summary of the results of the analysis of RNA-seq data, by running method 1.

See also Figures S1 and S2 and Tables S1–S3.

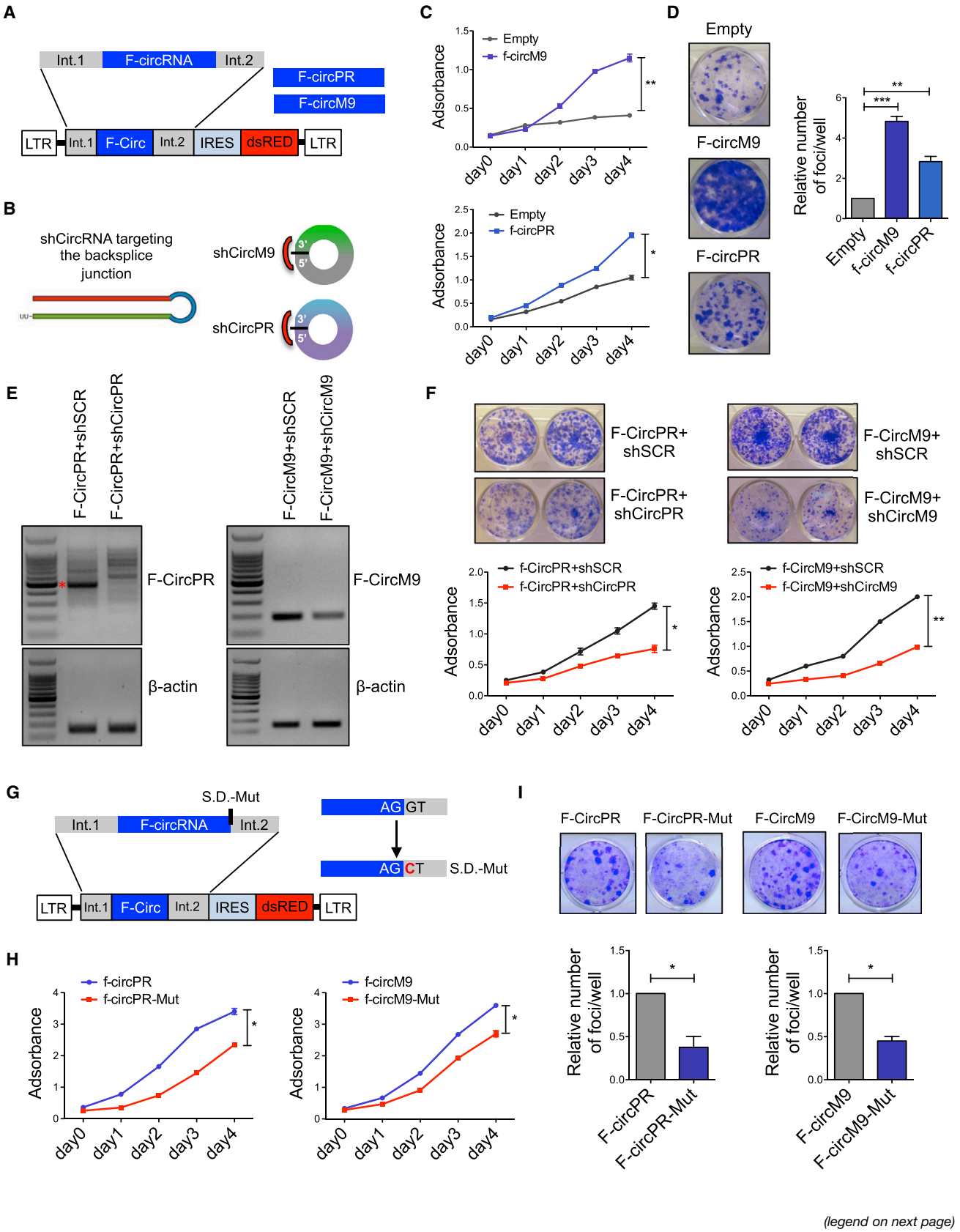

(legend on next page)

this analysis. Sanger sequence revealed that sarcoma cells displayed expression of f-circRNAs composed by *EWSR1* and its partner *FLI1* (f-circEF1), with the back-splice junction encompassing the 5′-head of *EWSR1* exon 7 and exon 10 of *FLI1* (Figures S2A and S2B). Similarly, lung cancer cell lines harboring the *EML4/ALK1* translocation (Figure S2C) showed the expression of a f-circRNA composed by *EML4* and *ALK1* (f-circEA1), with back-splice junction located between the 5′ head of *EML4* exon 12 and the 3′ tail of *ALK1* exon 26 (Figure S2D).

We next utilized an alternative approach for the identification of f-circRNAs. To this end, samples, whose expression of f-circRNAs was previously assessed by PCR, were submitted to RiboMinus-enriched RNA sequencing (RNA-seq) and next analyzed for the presence of reads spanning either the breakpoint region or the back-splice junction. We used two different approaches for the analysis of the f-circRNAs: method 1 and method 2. As reported in Figures S2E and S2F, method 1 consists of a single read mapping step, in which RNA-seq reads are directly mapped to the linear RNA fusion and f-circRNA fusion reference libraries using bowtie (Langmead et al., 2009). Next, among the mapped reads, reads containing the spliced junction of linear fusions and the back-spliced junction of f-circRNAs are identified. Finally, reads meeting the following three conditions are selected: (1) mapping to the f-circRNA or linear RNA fusion reference libraries, (2) containing the spliced or back-spliced junction, and (3) containing at least *w* bases per read from each gene involved in the fusion. We defined *w* as the minimum number of bases, which produced no false positive reads for the identification of linear fusion reads in both method 1 and method 2. We defined a false positive linear fusion read as the identification of a linear fusion read among cases not reported as containing the translocation (i.e., identification of a PML/RARα fusion transcript among a case reported as MLL/AF9). Method 2 consists of two read mapping steps. We first perform a filtering step to eliminate all RNA-seq reads that map to the human transcriptome downloaded from University of California, Santa Cruz (UCSC) reference data repository. (Guo et al., 2014; Memczak et al., 2013; Salzman et al., 2013). After this filtering step, the remaining unmapped reads are mapped to the linear RNA fusion and f-circRNA fusion reference libraries using bowtie, and linear fusion RNAs and f-circRNAs are identified using the same three conditions as in method 1 (See Tables S1–S3). The results obtained by the application of these pipelines are summarized in Figure 1G. Notably, for the identification of f-circRNAs, we counted only reads that span the back-splice junction of the f-circRNA, and we excluded all those reads that mapped shared sequences between the linear transcript and the f-circRNA. Thus, because of these strict bioinformatics criteria and the fact that the back-splice reads are by definition fewer than the shared reads from flanking sequences, the true prevalence of f-circRNAs in these samples may be higher than that reported in our analyses.

Taken together, the experiments and analysis show that chromosomal rearrangements affect the non-coding RNA dimension within tumor cells, particularly through the generation of f-circRNAs.

F-circRNAs Are Proto-oncogenic RNAs that Contribute to Cellular Transformation

Because translocations are early events in tumorigenesis and, in some circumstances, are the primary cause of the tumor onset, we investigated whether f-circRNAs themselves could play a functional role in this context. We sought to study the specific function of f-circRNAs with the goal of disentangling their possible activity from that of the concurrently present fusion protein in tumor cells. At first, we expressed f-circRNAs in immortalized, but not transformed, mouse embryonic fibroblasts (MEFs; see Experimental Procedures), which do not express the translocation and therefore do not express the fusion protein. Circularizing exons were then cloned into expressing vectors, together with up- and downstream flanking introns, in order to favor the spontaneous formation of the f-circRNAs (Figures 2A and S3A–S3C). The expression of f-circRNAs was assessed by qRT-PCR (Figure S3B) and PCR (Figure S3C) analysis of the specific back-splice junction of the f-circRNA. Importantly, expression of f-circRNA was then reverted for functional studies through the use of short hairpin circRNAs (shCircRNAs) targeting their back-splice junction (Figure 2B). f-circRNA-expressing cells were then compared to control cells (expressing an empty vector) for proliferation rate, loss of contact inhibition, and their transformed foci-forming capability. As shown in Figure 2C, cells expressing f-circPR and f-circM9_1 (from hereafter f-circM9 for brevity) both showed a higher proliferative rate when compared

Figure 2. F-circRNAs Are Oncogenic and Contribute to Cellular Transformation

(A) Schematic representation of the retroviral vectors used to express the f-circRNAs.

(B) Schematic representation of shCircRNAs used to target f-circRNAs at the back-splice junction.

(C) Proliferation curves of MEFs transduced with the empty vector (control) or with the vector expressing f-circM9 (upper panel) or f-circPR (lower panel). For each time point, the number of cells was detected by staining with crystal violet (n = 2 independent experiments, each performed in triplicate).

(D) Focus formation assay with MEFs cells expressing the empty vector, f-circM9 or f-circPR. Representative pictures are shown on the left, while the quantification of the foci per well is shown on the right. Error bars represent the mean ± SD (n = 2 independent experiments, each performed in triplicate).

(E) PCR detection of f-circPR and f-circM9 in MEFs expressing f-circPR or f-circM9 and then further transduced with shCircPR (left) or shCircM9 (right). The shSCR was used as control. The specific band is indicated (*).

(F) Proliferation rates of MEFs expressing f-circM9 or f-circPR and concomitantly transduced with shSCR, shCircM9, or shCircPR. Representative pictures are shown in the top, while the proliferation curves are shown in the bottom (n = 2 independent experiments, each performed in triplicate).

(G) Schematic representation of f-circRNA-Mut vectors, mutagenized at the splicing-donor site (SD).

(H) Proliferation rates of MEFs transduced with the f-circRNA-Mut vectors or expressing either f-circM9 (right) or f-circPR (left). The number of cells was detected upon staining with crystal violet (n = 3 independent experiments, each performed in triplicate).

(I) Focus formation assay performed with MEFs expressing f-circRNA-Mut vectors or either f-circM9 (right) or f-circPR (left). Representative pictures are shown in the top, while the quantification of the number of transformed foci per well is shown in the bottom (n = 3 independent experiments, charts show the mean ± SEM). See also Figure S3.

to cells expressing the empty vector. Accordingly, their ability to form foci characterized by loss of contact inhibition was much higher compared to control cells (Figure 2D; see Experimental Procedures), suggesting that f-circRNAs are indeed functional and tumor promoting. In order to confirm these results, we next silenced the expression of f-circRNAs by transducing cells with shCircRNAs spanning the f-circRNA back-splice junction (Figure 2E). Intriguingly, the increased proliferation rate observed in cells expressing f-circRNAs was reverted upon the silencing of the f-circRNAs (Figure 2F), corroborating the notion that these f-circRNAs (both for f-circPR and f-circM9) exert tumor promoting activity in immortalized MEFs and are involved in the tumorigenic process independent of their linear transcript and their fusion protein counterparts.

In order to obtain additional and independent support of the functionality of f-circRNAs, we next adopted an alternative experimental strategy. f-circRNAs-expressing vectors were mutagenized at the splicing donor site (f-circRNA-mut), following a strategy already reported in (Wang and Wang, 2015) and as shown in Figure 2G. f-circRNA-mut vectors allowed the expression of the linear transcript, while impairing the circularization event (Figures 2G and S3D). Immortalized MEFs were then transduced with either f-circRNA-mut vectors or regular f-circRNAs-expressing vectors, and the cells' proliferation and transformation were then assayed. In line with our previous experiments, the expression of f-circRNAs (both for f-circPR and f-circM9) triggered cells to increase their proliferation rate and to form foci, if compared to the expression of f-circRNA-mut vectors (Figures 2H and 2I).

We next tested whether the expression of f-circPR and f-circM9 would lead to the activation of common or distinct proto-oncogenic pathways. Intriguingly, although the expression of f-circPR and f-circM9 showed similar biological outcomes in MEFs, we found that they triggered differentially the activation of the PI3K and MAPK signal transduction pathways (Figures S3E and S3F). This in turn suggests that f-circRNAs may exert their tumorigenic activity through distinct signaling outputs.

Together, these experiments reveal that f-circPR and f-circM9 are biologically active, exerting pro-proliferative and proto-oncogenic activities.

F-circRNAs Contribute to Leukemia Progression In Vivo

Experiments performed with immortalized MEFs allowed an initial evaluation of the possible involvement of f-circRNAs in cellular transformation. In order to directly test the role of f-circRNAs in tumor cells in vivo, we utilized primary hematopoietic cells and set up the conditions to study the involvement of f-circRNAs during the onset and progression of leukemia. We decided to focus our work on the MLL/AF9-AML model, and using this model, we investigated the role of f-circM9. At first we set to address the question on whether f-circM9 alone was sufficient to trigger leukemia from hematopoietic stem cells (HSCs). To investigate, HSCs were isolated from wild-type mice, transduced in vitro with a vector expressing f-circM9 (or an empty vector as control), and used for either in vitro methyl-cellulose assays or transplanted back into sub-lethally irradiated recipients. Regardless of the expression of f-circM9, HSCs differentiated during the methyl-cellulose cultures toward exhaustion (data not shown). Similarly, none of the transplanted mice developed leukemia following the transplantation of the infected cells in a 3-months follow up, and only very few donor-derived cells were found in the BM of transplanted mice (data not shown). These initial experiments suggested that f-circM9 is probably not sufficient to trigger tumorigenesis on its own, and additional oncogenic events might be required.

Because at the onset of chromosomal translocations, the formation of f-circRNAs is always coupled with the presence of f-Linear RNAs and the encoded oncogenic fusion proteins, which have been already described as fundamental hits for the tumorigenesis process, we decided to investigate the relevance of f-circM9 in the presence of the MLL/AF9 fusion protein. HSCs were therefore transduced with a GFP-labeled retroviral vector, which expressed the cDNA of MLL/AF9, as described in Figure S4A. Infected cells were then transplanted in sub-lethally irradiated mice. This vector expressed the fusion protein and triggered a pre-leukemic phase. After 2 months from the transplantation, mice started to develop leukemia, accordingly to what has been previously reported (Krivtsov and Armstrong, 2007). GFP+ leukemic cells were then sorted out from recipient mice and transduced in vitro, either with an empty vector or the f-circM9-expressing vector (Figures 3A and 3B). As a further control, in an independent experimental setting, leukemic cells were also transduced with the f-circM9-expressing vector or the f-circM9-Mut-expressing vector (Figures 3A–C). Cells expressing these vectors were re-sorted as dsRED+ cells and used for in vitro and in vivo experiments. Sorted cells were then plated in vitro in methyl-cellulose. After 5 days in culture, proliferation and the capacity to form colonies were evaluated. At the point of colony count, cells were then re-suspended and used for a second round of methyl-cellulose assay. As shown in Figure 3D, cells expressing f-circM9 together with the MLL/AF9 fusion protein displayed an increased ability to proliferate and form colonies in serial plating when compared to cells expressing solely the MLL/AF9 fusion protein. Similar results were obtained in the other experimental setting: MLL/AF9-positive cells transduced with the f-circM9 showed proliferative advantage and a higher colony-formation capacity when compared to cells transduced with the f-circM9-Mut vector, which was deficient for the formation of the f-circM9 (Figure 3E).

These ex vivo experiments contributed to strengthening the hypothesis that f-circRNAs could contribute to the leukemogenic process. To obtain in vivo evidence of their role in leukemogenesis, we next performed transplantations experiments. GFP+ leukemic cells (already expressing MLL/AF9 cDNA) were transduced with f-circM9 or f-circM9-Mut vectors, re-sorted as dsRED+ cells, and then transplanted into sub-lethally irradiated mice. In order to study the contribution of the f-circM9 to leukemogenesis at the single-cell level, transplantations were performed with different cell numbers and in a limiting-dilution setting, transplanting either 30,000 or 500 cells per recipient. 3 weeks after transplantation, recipient mice were sacrificed, the expression of f-circM9 in leukemic cells was confirmed by PCR, and the progression of leukemia was analyzed. No difference in the number of leukemic blasts was detected in mice transplanted with a high number of leukemic cells. Irrespective of the expression of the f-circM9, mice developed leukemia and displayed similar percentages of leukemic cells within

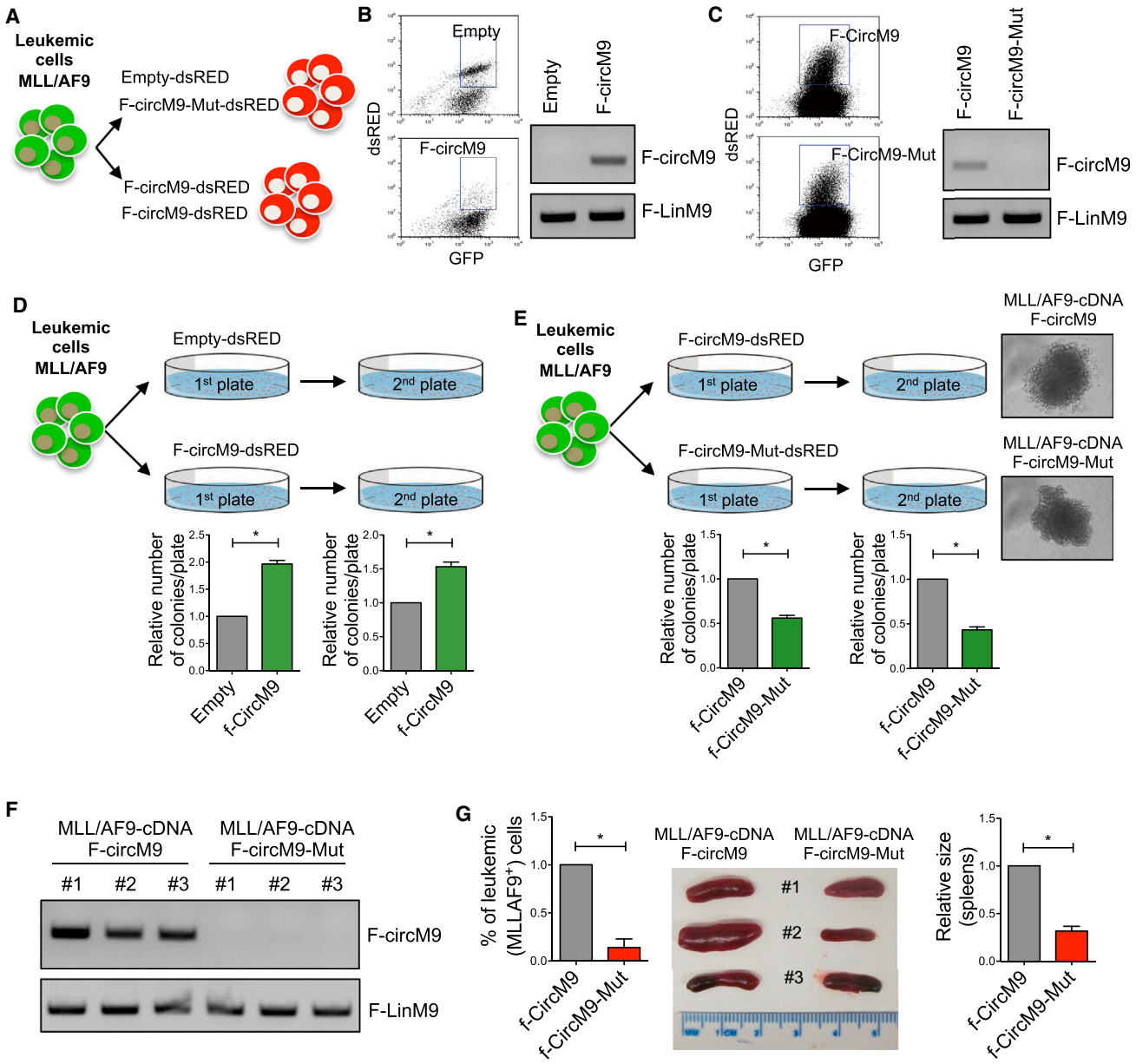

Figure 3. F-circM9 Is Oncogenic and Contributes to Leukemia Progression

(A) Schematic representation of the generation of leukemic cells that express concomitantly MLL/AF9 fusion protein and f-circM9.

(B) Isolation and validation of leukemic cells that express the fusion protein MLL/AF9 (GFP+ cells) and further transduced with the vector expressing f-circM9 or empty vector (dsRED$^+$ cells).

(C) Isolation and validation of leukemic cells that express the fusion protein MLL/AF9 (GFP+ cells) and further transduced with the f-circM9-Mut vector or the vector expressing f-circM9 (dsRED$^+$ cells).

(D) Methyl-cellulose assays performed with leukemic cells (MLL/AF9-GFP fusion protein) expressing either the empty vector or f-circM9. Two rounds of re-plating have been performed. Charts represent the quantification of the number of colonies per plate (n = 3 independent experiments; error bars represent the mean ± SD).

(E) Methyl-cellulose assays performed with leukemic cells (MLL/AF9-GFP fusion protein) expressing either the f-circM9-Mut vector or f-circM9. Two rounds of re-plating have been performed. Charts represent the quantification of the number of colonies per plate (n = 2 independent experiments; error bars represent the mean ± SD).

(F) PCR analysis of leukemic cells derived from transplanted mice, for the expression of f-circM9 or LinM9 (n = 3 mice each group).

(G) Analysis of the recipient mice transplanted with leukemic cells (that carry the MLL/AF9 fusion protein) transduced with f-circM9-Mut vector or expressing f-circM9. The percentage of leukemic cells in the bone marrow (BM) is shown on the left, pictures of the spleens of the recipient mice are shown in the middle panel, while the size is shown in the chart on the right. Error bars represent the mean ± SEM (n = 3 mice per group).

See also Figure S4.

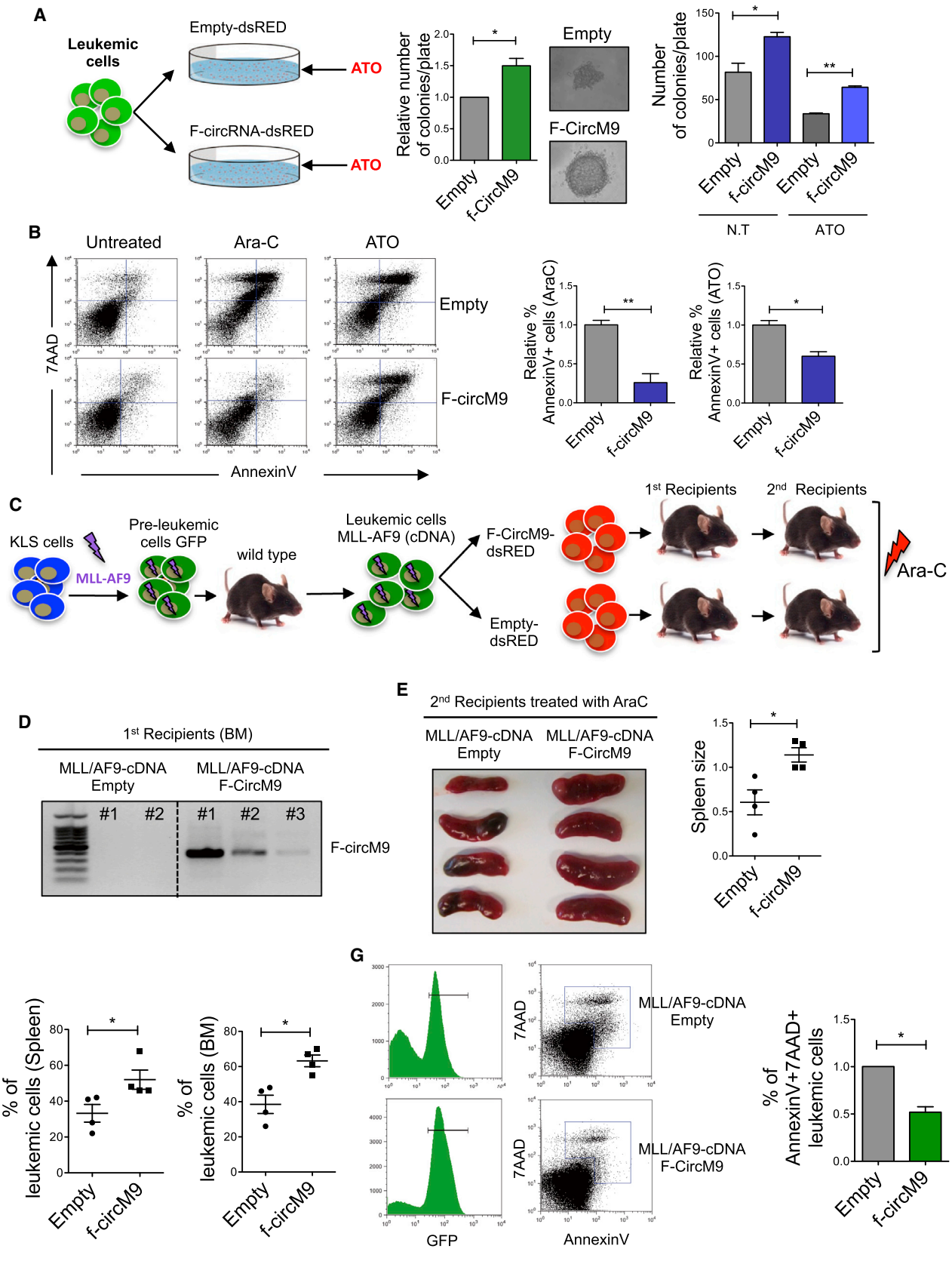

(legend on next page)

spleen and BM (Figure S4B). Interestingly, however, when transplanted at limiting rate, clear differences could be observed between the recipient mice (Figures 3F and 3G). The presence of the f-circM9 favored the progression of the leukemia. Within 3 weeks, mice that were transplanted with leukemic cells carrying the f-circM9 together with the MLL/AF9 fusion protein (Figure 3F) showed an enlarged spleen and a higher number of leukemic cells both in the BM and spleen (Figure 3G).

All together, these data support the notion that f-circM9, when coupled with other oncogenic stimuli (e.g., the presence of the oncogenic fusion protein), plays an active role in favoring leukemia progression in vivo.

F-circRNAs Confer Resistance to Therapy In Vivo

Disease relapse following transient remission achieved with conventional and targeted therapies still remains one of the central problems in the treatment of leukemia (Bailey et al., 2008; Forman and Rowe, 2013). Relapse is often associated with the development of resistance to therapy and thus loss of responsiveness to further treatment (Ding et al., 2012; Zahreddine and Borden, 2013). Since the expression f-circRNAs confers a proliferative advantage to leukemic cells, we next investigated the possibility that the expression of f-circRNA could also confer a survival advantage and protection to cancer cells from drug-induced apoptosis. To answer this important question, we performed in vitro and in vivo experiments in the MLL/AF9 model. Leukemic cells carrying the MLL/AF9 fusion protein were transduced with f-circM9 or an empty vector. For in vitro experiments, cells were sorted as dsRED+ and cultured in methyl-cellulose. Arsenic trioxide (ATO) (Ito et al., 2008), an approved standard-of-care drug for the treatment of leukemia, was then added to the semi-solid medium; cells were cultured for 5 days, and proliferation and colony formation were assessed. As shown in Figure 4A, the presence of f-circM9 conferred protection to leukemic cells upon treatment. Increase in the size and number of colonies was observed at the end of the treatment for cells expressing the f-circM9, as compared to those infected with the control vector (Figures 4A and S5A).

To corroborate these results, we used, in an independent experimental setting, an additional standard-of-care approved drug for leukemia treatment: cytarabine (Ara-C), (Löwenberg et al., 2011) (Lengfelder et al., 2012). K562 cells (Lozzio and Lozzio, 1979) were then transduced with viral vectors expressing f-circM9; cells transduced with the empty vector were used as control. F-circM9-expressing cells were sorted for a pure population and were subsequently subjected to treatment with Ara-C and ATO. As shown in Figure 4B, no differences in apoptosis were detected upon the expression of f-circRNAs in untreated cells. On the contrary, clear differences were noticed upon treatment. Cells transduced with the empty vector showed signs of apoptosis upon treatment with either Ara-C or ATO, while cells expressing f-circM9 showed to be markedly protected and displayed reduced signs of apoptosis. These results further demonstrate that f-circM9 can bestow to tumor cells a survival advantage in response to therapy treatment, hence likely impacting therapeutic outcomes.

Next, to further validate whether f-circM9 could confer protection to leukemic cells under treatment, we performed in vivo experiments. In order to get a sufficient number of cells to perform the experiment, we expanded leukemic cells expressing either f-circM9 or the empty vector in primary recipients (Figure 4C). The expression of the transgene was found to be maintained throughout the entire experiment (Figure 4D). The same number of leukemic cells were then derived from primary recipients and transplanted into experimental mice (Figure 4C, secondary recipients). After the onset of leukemia (2 weeks after the transplantation) mice were treated with Ara-C as described (Zuber et al., 2009). 4 days post-treatment, mice were sacrificed, and leukemia progression was analyzed. As shown in Figure 4E, mice transplanted with leukemic cells that expressed f-circM9 showed enlarged spleens compared to mice transplanted with leukemic cells of control. Importantly, the number of leukemic cells infiltrating the spleen and the BM was higher in the f-circM9-expression setting compared to the control setting (Figure 4F).

Because the number of surviving cells in the treatment with chemotherapy was higher where the leukemic cells expressed the f-circM9 together with the MLL/AF9 fusion protein, we also sought to investigate their levels of apoptosis. To this end, we stained leukemic cells within the BM with AnnexinV-7AAD. The overall number of apoptotic leukemic cells (GFP+) after treatment was reduced in mice bearing leukemic cells that expressed f-circM9, as compared to the controls (Figure 4G). These results further demonstrate that f-circRNAs originating from chromosomal translocation are functionally active and can provide

Figure 4. Expression of f-circM9 in Cancer Cells Confers Resistance to Treatments

(A) Methyl-cellulose assays performed with leukemic cells expressing f-circM9 and in the presence of ATO. Schematic representation of the assay is shown on the left, the relative number of colonies upon the treatment with ATO and their morphology are shown in the middle panel, while the absolute number of colonies is shown on the right. NT, not treated (n = 3 independent experiments; charts show mean ± SEM).

(B) Analysis of apoptosis of K562 cells expressing f-circM9 and treated either with Ara-C or ATO. Representative plots are shown on the left, while the quantification of AnnexinV$^+$ cells is shown on the right (n = 3 independent experiments; charts show mean ± SEM).

(C) Schematic representation of the in vivo assay to study the involvement of f-circM9 in conferring protection to cancer cells upon treatment with chemotherapy.

(D) Expression of f-circM9 in leukemic cells in the BM of primary recipient mice.

(E) Analysis of the size of the spleens of secondary recipient mice transplanted with leukemic cells (MLL/AF9 fusion protein) expressing the f-circM9 (or the empty vector) and treated with AraC.

(F) Percentage of leukemic cells in the spleen (left) and in the BM (right) of secondary recipient mice transplanted with leukemic cells (MLL/AF9 fusion protein) expressing the f-circM9 and treated with AraC.

(G) Analysis of apoptosis of leukemic cells (that carry the MLL/AF9 fusion protein) expressing f-circM9 (or the empty vector) in mice treated with Ara-C. Cells positive for the expression of AnnexinV and 7AAD have been analyzed within the GFP+ population of leukemic cells. Representative plots are shown on the left, while the quantification as mean ± SEM is shown on the right.

See also Figure S5.

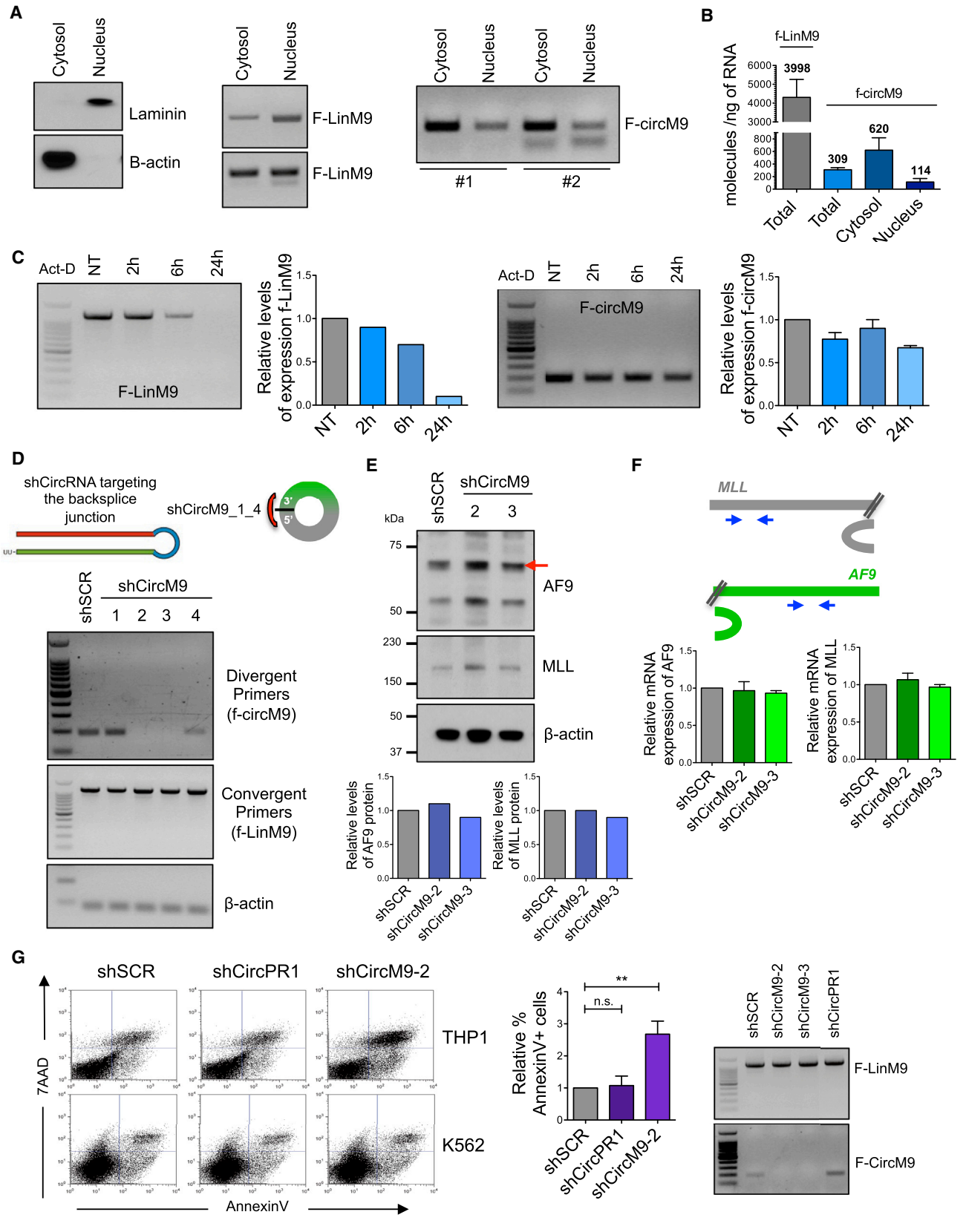

(legend on next page)

tumor cells a survival advantage in response to therapy treatment, likely impacting therapeutic outcomes.

F-circRNAs Are Critical for Human Leukemic Cells Viability

While the experiments we have performed demonstrate a role for f-circRNAs in cellular transformation and tumor progression, we next assessed whether the expression of the endogenous f-circRNAs is relevant to the survival of human leukemic cells that endogenously carry the chromosomal translocation.

To this end, we first analyzed the expression, the subcellular distribution, and stability of one of the two endogenous f-circM9s (f-circM9_1) (Figure 1F) in THP1 cells, and then we performed functional experiments aimed at knocking down the endogenous f-circM9_1. In order to determine the localization of f-circM9_1, we fractionated cells in cytosolic and nuclear fractions, and the presence of f-circM9_1 was assessed in each fraction as number of molecules of f-circM9_1 per ng of total RNA (Figures 5A–5C). THP1 cells expressed lower levels of f-circM9_1 if compared to its linear-fusion transcript. Interestingly, we observed the presence of f-circM9_1 in both cytosolic and nuclear compartments, with enrichment in the cytosol, as compared to the nuclear fraction (Figures 5A and 5B). Moreover, when compared to its linear transcripts, f-circM9_1 showed higher stability (Figure 5C), in agreement to what was already reported about other circRNAs (Jeck et al., 2013).

We next targeted f-circM9_1 using shRNAs specifically directed against the back-splice junction. We screened different shCircRNAs in order to find a candidate that: (1) has the ability to knock down the f-circM9_1 (assessed by PCR with divergent primers) (Figure 5D), (2) does not effect the linear transcripts and the MLL and AF9 proteins (assessed by western blot, Figure 5E, and by PCR using primers that can selectively recognize the linear transcripts, Figure 5F), and (3) has no toxic effects on unrelated cells (assessed by testing the shCircRNAs on leukemic cell lines that do not carry the MLL/AF9 translocation, Figures 5G and S6E). Only one of the screened shCircRNAs (shCircM9-2) met all the three criteria and was therefore used to evaluate the functionality of f-circM9_2 in THP1 cells (Figure 5G). The knock down of f-circM9 in THP1 cells resulted in increased apoptosis, as measured with the AnnexinV-7AAD staining (Figure 5G). We used a similar approach to identify a shCircRNA effectively targeting f-circPR (Figures S6A–S6E). The knockdown of f-circPR in NB4 cells also triggered apoptosis, while increasing the expression of p21 and p27 compared to control cells (Figure S6F). Thus, f-circRNAs play an important role in maintaining the viability of leukemic cells.

DISCUSSION

Genomic alterations, particularly aberrant chromosomal translocations, are responsible for the onset of many types of cancers, like leukemia, as well as solid tumors (Rabbitts, 1994) (Bunting and Nussenzweig, 2013). How such rearrangements can lead to tumorigenesis has been explained by their ability to encode and express oncogenic proteins. However, whether such alterations of the genome could also simultaneously impact the non-coding RNA dimension has been poorly explored to date. Here, we investigated whether chromosomal translocations could affect the circRNA's dimension of cancer cells. This analysis allowed us to reach several important conclusions:

Chromosomal Translocations Generate Aberrant F-circRNAs

The biogenesis of these circRNAs is favored by the juxtaposition of otherwise-separated complementary intronic sequences up- and downstream of the breakpoint region of the translocation (Figure 6A). According to the presence of such complementary regions within the introns that are located next to the breakpoint, all of the fused primary mRNAs derived from chromosomal translocations, in frame or out of frame, may potentially give rise to f-circRNAs (Jeck et al., 2013). Initiation analysis of a few chromosomal translocations occurring in various tumor types revealed that f-circRNAs are generated in 50% of cases. Thus, many other chromosomal translocations in addition to PML/RARα, MLL/AF9, EWSR1-FLI1, and EML4/ALK1 described here might generate f-circRNAs. F-circRNAs could be also generated from the multitude of out-of-frame chromosomal translocations observed in human cancer, which have not been functionally characterized in view of the lack of protein coding capability. Furthermore, we show that, as described for circRNAs in normal cells from different tissues, multiple combinations of circularizing exons can be generated from the same fusion gene. On this basis, high-throughput bioinformatics platforms should be developed to identify f-circRNAs derived from all known chromosomal translocations.

Notably, recent reports have shown that circRNAs can be stably secreted in exosomes (Li et al., 2015c) and therefore utilized

Figure 5. Analysis of the Endogenous f-circM9 and its Role in the Maintenance of Cancer Cells

(A) Fractionation nucleus/cytoplasm of THP1 and analysis of f-LinM9 and f-circM9 within each fraction. Western blot analysis of laminin and beta-actin is shown on the left.

(B) Quantification of LinM9 and f-circM9 in the total RNA, nuclear RNA, or cytosolic RNA of THP1 cells. Charts are shown as mean of the replicates ± SEM.

(C) Analysis of the stability of LinM9 (left) and f-circM9 (right) in THP1 cells treated with Actinomycin-D. Error bars represent the mean ± SD.

(D) shCircM9_1_4 targeting the back-splice junction are used to knock down the f-circM9. The efficiency is measured by PCR. Convergent primers are used to detect the LinM9, while divergent primers are used to detect the f-circM9.

(E) Western blot analysis of endogenous MLL and AF9 proteins in THP1 cells upon transduction with shCircM9 vectors. The quantification of the bands is shown on the lower panel.

(F) Schematic representation (top) of the primers (not included in the f-circM9) used to identify MLL and AF9 transcripts. Lower charts show the expression of MLL and AF9 mRNAs as mean ± SD.

(G) Apoptosis of THP1 cells transduced with shCircPR or shCircM9. Representative plots are shown on the left, while the quantification of the AnnexinV+ cells is shown on the right. Error bars represent the mean of the replicates ± SEM. PCR assay on the right shows the efficacy of the knockdown.

See also Figure S6.

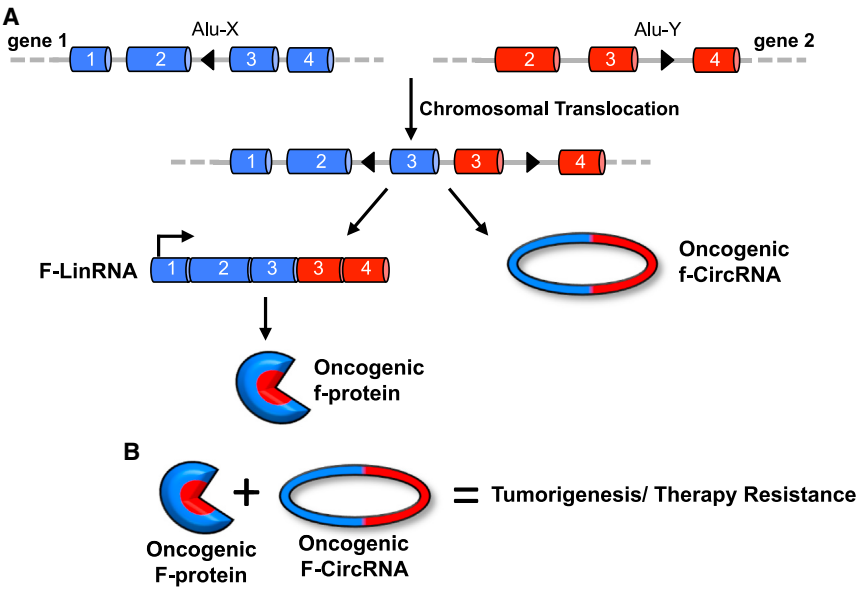

Figure 6. Biogenesis and Role of F-circRNAs in Tumor Progression

(A) Schematic representation of the origin of f-circRNAs from chromosomal translocations and their co-existence with oncogenic fusion-proteins in tumor cells.

(B) Schematic representation of the role of f-circRNAs in tumor progression and resistance to therapy.

as diagnostic and prognostic markers for cancer (Bahn et al., 2015; Li et al., 2015b; Salzman et al., 2012). In this respect, f-circRNAs in secreted exosomes could be used as pathognomonic markers for many tumor types, especially for those whose biopsies are difficult to obtain.

Additionally, although not investigated in the present work, chromosomal translocation events can also "knock out" circRNAs normally generated from the wild-type loci involved in the translocation, when these circRNAs encompass the breakpoint region. A deeper investigation of these "inactivating" events and their functional consequences could be just as informative in revealing new tumor-suppressive players involved in the onset and progression of the disease.

Aberrant F-circRNAs Are Functionally Relevant During Cancer Development and Are Tumor Promoting

We demonstrated that f-circRNAs, together with other oncogenic hits, are able to increase cellular proliferation rate and contribute to cellular transformation and tumorigenesis both in vitro as well as in vivo. These findings uncover a new layer of complexity underlying the role of chromosomal translocations in human disease pathogenesis, whereby the biological outputs, in this case the oncogenic signals, might be not be solely limited to the encoded fusion proteins. In this "multiple hits in one" scenario, the concomitant expression in tumor cells of linear fusion mRNAs (exerting a possible non-coding RNA function), fusion-proteins, and f-circRNAs could be, in some instances, critical for tumor onset and progression (Figure 6B). These findings have a number of relevant corollary implications. Experimental models that mimic the presence of the translocation only by the expression of the related protein might not completely phenocopy the human disease, in turn explaining the long latency often observed in mouse models of cancer. Thus, in such models, biological mechanisms relevant to tumorigenesis might be missed. Second, and importantly, in all of the cases of out-of-frame chromosomal translocations, the generation of f-circRNAs could represent a functionally relevant oncogenic element, leading to tumor development, independent of the fusion protein.

The Expression of F-circRNAs in Cancer Cells Is Essential for Their Maintenance and Confers Resistance to Therapy

We demonstrate that, upon silencing of endogenous f-circRNAs, cancer cells undergo apoptosis, while f-circM9 expression protects cancer cells from drug-induced apoptosis. On this basis, a deeper characterization of the mechanisms of such resistance is needed to identify new therapeutic targets, and pharmaceutical interventions that are aimed at blocking f-circRNAs or their down-stream effectors could prove beneficial, when paired with conventional therapies, to eradicate the disease.

The mechanisms of action of f-circM9 might however be distinct and not be shared with other f-circRNAs. Although the expression of both f-circPR and f-circM9 leads to increased cellular proliferation and transformation, different cellular pathways are switched on. Mitogen-activated protein kinase (MAPK)- and AKT1-induced signals are simultaneously triggered by the presence of f-circM9, while on the contrary, only a slight increase of the p-AKT is observed in the presence of f-circPR. These data suggest that each f-circRNA might exert a unique biological function through distinct mechanisms of action within cancer cells.

Collectively our work demonstrates the existence of f-circRNAs and their relevance to human disease. Our observations expand on the current knowledge about the onset and progression of cancer and unravel new possible opportunities for therapeutic intervention. The systematic identification and characterization of f-circRNAs might therefore represent an important step in the understanding of the genetic and molecular basis of cancer development.

EXPERIMENTAL PROCEDURES

Cell Lines and Reagents

THP-1, K562, U937, HL-60, Kasumi, and NB4 cell lines were maintained in RPMI medium with 10% FBS. Arf−/− MEFs (early passages) were grown in DMEM 10% FBS. Primary leukemic cells were maintained in StemSpan (Stem Cell Technologies) supplemented with IL6 (15 ng/mL), IL3 (15 ng/mL) TPO (50 ng/mL) and SCF (50 ng/mL). Cells were grown at 37°C in a 5% CO_2 humidified incubator. In selected experiments, cells were treated with arsenic

trioxide (ATO) 0.1 μM for primary cells and 1 μM for K562 or with cytarabine (Ara-C) 0.5 μM.

Mice

Animal experiments were performed in accordance with the guidelines of Beth Israel Deaconess Medical Center Institutional Animal Care and Use Committee. For limiting-dilution experiments (Figures 3F and 3G), leukemic cells were transduced with retroviral vectors and then re-sorted for dsRED (Figure 3A). Sorted cells were then injected into sub-lethally irradiated recipients at a concentration of 500 cells/mouse or 30,000/mouse; mice were sacrificed and analyzed 3 weeks after. For treatment experiments, Ara-C was administered daily for 4 days, at the concentrations published in Zuber et al. (2009).

Isolation of RNA, Treatment with RNase-R, and PCR

Total RNA was extracted using TRIZOL (Invitrogen) according to the manufacturer's instructions. RNase-R treatment was carried out for 15 min at 37°C using RNase-R (Epicenter) 2 U/μg. Treated RNA was directly reverse transcribed using the RETROscript System (Life Technologies) with random decamer primers. 40 ng of RNA were used for the PCR analysis of the f-circRNAs. The PCR reactions were performed using HotStarTaq Master Mix (QIAGEN) for up to 40 cycles. Primer sequences are provided in Table S4. PCR products were visualized after electrophoresis in a 1.5% agarose gel. For sequencing, PCR products were purified from the gel by using the QIAquick extraction kit (QIAGEN). In selected experiments, qRT-PCRs were carried out using SybrGreen reaction mix and StepOnePlus real-time PCR system (Applied Biosystems). LinM9 and f-circM9 were quantified by PCR, in respect to their standard curve. In order to generate the standard curve, the PCR products containing the back-splice junction (for f-circM9) or the break point (for the LinM9) were cloned using the pGEM-T easy Vector System II (Promega), by following the manufacturer instruction. The number of molecules was then calculated by quantifying the PCR bands of f-circRNA or LinRNA, and by plotting them to the serially diluted standard curve.

Western Blots

Cell lysates were prepared with RIPA buffer. The following antibodies were used: rabbit anti-PML clone H-238 (Santa Cruz), rabbit polyclonal anti-RARα (Santa Cruz), mouse polyclonal anti-β-actin (Sigma-aldrich), mouse monoclonal anti-HSP90 (BD Biosciences), anti-AF9 (Bethyl), anti-MLL (Bethyl), anti-Akt (Cell Signaling), anti-pAkt (S473) (Cell Signaling), anti-ERK1/2 (Cell Signaling), and anti-pERK1/2 (Cell Signaling).

Proliferation Assays, Crystal Violet Staining, and Focus Formation Assay

MEFs were derived from p19-Arf$^{-/-}$ mice and immortalized in culture by culturing for several passages. For the proliferation assay, cells were seeded at a concentration of 5 × 10^4 cells per well in a 12-wells plate and cultured for 5 days in complete medium (DMEM + 10% FBS) at 37°C. Cells were then fixed every day and stained with crystal violet. For the focus formation assay, cells were seeded at a concentration of 5 × 10^4 cells per well in a 12-wells plate, and the cultures were carried on for 10 days without changing media. Once formed, the visible cell foci were fixed with 10% formalin for 30 min and subsequently stained with crystal violet. Crystal violet was then solubilized with 10% acetic acid, and their absorbance was measured.

Flow-Cytometry Analysis of Annexin-V$^+$ Cells

Apoptotic cells were analyzed with 7AAD and Annexin-V-APC. Cells were stained for 15 min with both markers and then analyzed using LRSII (BD, PharMingen).

Bioinformatics Analysis

Total RNA-seq data from one set of THP1 cell line was downloaded from the GEO (Barrett et al., 2013) under accession number GSM1125252. For all the other samples, ribo-minus enriched RNA-seq data of cell lines (THP1 s set and NB4) and primary patients with acute leukemia harboring PML/RARα fusion gene (APL_1-4) was run at the Center for Cancer Computational Biology (CCCB) at the Dana-Farber Cancer Institute. The accession number for the RNA-seq reported in this paper is BioProjectID: PRJNA315254.

ACCESSION NUMBERS

The accession numbers for the linear fusion sequences, MLL/AF9 and PML/RARα, reported in this paper is NCBI: EF406122 and AB067754, respectively.

SUPPLEMENTAL INFORMATION

Supplemental Information includes Supplemental Experimental Procedures, six figures, and six tables and can be found with this article online at http://dx.doi.org/10.1016/j.cell.2016.03.020.

AUTHOR CONTRIBUTIONS

J.G., M.B., and P.P.P. designed, realized, and analyzed the experiments. J.C.J. and A.H.B. performed the bioinformatics analysis, S.V.P., K.B., M.M.N., and Y.T helped with the experiments. F.L.-C. provided human APL samples. J.G. and P.P.P. wrote the manuscript.

ACKNOWLEDGMENTS

We thank Lauren Southwood and Kaitlyn Doherty for insightful editing and all members of the Pandolfi lab for critical discussion. We thank Dr. Daniel Costa for providing H3122 cell line and Dr. Mireia Castillo Martin for providing SKNEP cell line. J.G. was supported by a fellowship from American- Italian Cancer Foundation during the execution of this work. S.V.P. has been granted leave of absence from the German Cancer Research Center DKFZ, Heidelberg.

Received: September 6, 2015
Revised: December 18, 2015
Accepted: March 10, 2016
Published: March 31, 2016

REFERENCES

Anderson, J.L., Denny, C.T., Tap, W.D., and Federman, N. (2012). Pediatric sarcomas: translating molecular pathogenesis of disease to novel therapeutic possibilities. Pediatr. Res. *72*, 112–121.

Ashwal-Fluss, R., Meyer, M., Pamudurti, N.R., Ivanov, A., Bartok, O., Hanan, M., Evantal, N., Memczak, S., Rajewsky, N., and Kadener, S. (2014). circRNA biogenesis competes with pre-mRNA splicing. Mol. Cell *56*, 55–66.

Bahn, J.H., Zhang, Q., Li, F., Chan, T.M., Lin, X., Kim, Y., Wong, D.T., and Xiao, X. (2015). The landscape of microRNA, Piwi-interacting RNA, and circular RNA in human saliva. Clin. Chem. *61*, 221–230.

Bailey, L.C., Lange, B.J., Rheingold, S.R., and Bunin, N.J. (2008). Bone-marrow relapse in paediatric acute lymphoblastic leukaemia. Lancet Oncol. *9*, 873–883.

Barrett, T., Wilhite, S.E., Ledoux, P., Evangelista, C., Kim, I.F., Tomashevsky, M., Marshall, K.A., Phillippy, K.H., Sherman, P.M., Holko, M., et al. (2013). NCBI GEO: archive for functional genomics data sets–update. Nucleic Acids Res. *41*, D991–D995.

Barrett, S.P., Wang, P.L., and Salzman, J. (2015). Circular RNA biogenesis can proceed through an exon-containing lariat precursor. eLife *4*, e07540.

Bunting, S.F., and Nussenzweig, A. (2013). End-joining, translocations and cancer. Nat. Rev. Cancer *13*, 443–454.

Calin, G.A., and Croce, C.M. (2007). Chromosomal rearrangements and microRNAs: a new cancer link with clinical implications. J. Clin. Invest. *117*, 2059–2066.

Cheetham, S.W., Gruhl, F., Mattick, J.S., and Dinger, M.E. (2013). Long noncoding RNAs and the genetics of cancer. Br. J. Cancer *108*, 2419–2425.

Chin, L., Hahn, W.C., Getz, G., and Meyerson, M. (2011). Making sense of cancer genomic data. Genes Dev. *25*, 534–555.

Conn, S.J., Pillman, K.A., Toubia, J., Conn, V.M., Salmanidis, M., Phillips, C.A., Roslan, S., Schreiber, A.W., Gregory, P.A., and Goodall, G.J. (2015). The RNA binding protein quaking regulates formation of circRNAs. Cell *160*, 1125–1134.

Croce, C.M. (2009). Causes and consequences of microRNA dysregulation in cancer. Nat. Rev. Genet. *10*, 704–714.

Dekking, E.H., van der Velden, V.H., Varro, R., Wai, H., Böttcher, S., Kneba, M., Sonneveld, E., Koning, A., Boeckx, N., Van Poecke, N., et al.; EuroFlow Consortium (EU-FP6, LSHB-CT-2006-018708) (2012). Flow cytometric immunobead assay for fast and easy detection of PML-RARA fusion proteins for the diagnosis of acute promyelocytic leukemia. Leukemia *26*, 1976–1985.

Ding, L., Ley, T.J., Larson, D.E., Miller, C.A., Koboldt, D.C., Welch, J.S., Ritchey, J.K., Young, M.A., Lamprecht, T., McLellan, M.D., et al. (2012). Clonal evolution in relapsed acute myeloid leukaemia revealed by whole-genome sequencing. Nature *481*, 506–510.

Dos Santos, G.A., Kats, L., and Pandolfi, P.P. (2013). Synergy against PML-RARa: targeting transcription, proteolysis, differentiation, and self-renewal in acute promyelocytic leukemia. J. Exp. Med. *210*, 2793–2802.

Forman, S.J., and Rowe, J.M. (2013). The myth of the second remission of acute leukemia in the adult. Blood *121*, 1077–1082.

Greuber, E.K., Smith-Pearson, P., Wang, J., and Pendergast, A.M. (2013). Role of ABL family kinases in cancer: from leukaemia to solid tumours. Nat. Rev. Cancer *13*, 559–571.

Guo, J.U., Agarwal, V., Guo, H., and Bartel, D.P. (2014). Expanded identification and characterization of mammalian circular RNAs. Genome Biol. *15*, 409.

Hansen, T.B., Jensen, T.I., Clausen, B.H., Bramsen, J.B., Finsen, B., Damgaard, C.K., and Kjems, J. (2013). Natural RNA circles function as efficient microRNA sponges. Nature *495*, 384–388.

Hsu, M.T., and Coca-Prados, M. (1979). Electron microscopic evidence for the circular form of RNA in the cytoplasm of eukaryotic cells. Nature *280*, 339–340.

Ito, K., Bernardi, R., Morotti, A., Matsuoka, S., Saglio, G., Ikeda, Y., Rosenblatt, J., Avigan, D.E., Teruya-Feldstein, J., and Pandolfi, P.P. (2008). PML targeting eradicates quiescent leukaemia-initiating cells. Nature *453*, 1072–1078.

Jeck, W.R., and Sharpless, N.E. (2014). Detecting and characterizing circular RNAs. Nat. Biotechnol. *32*, 453–461.

Jeck, W.R., Sorrentino, J.A., Wang, K., Slevin, M.K., Burd, C.E., Liu, J., Marzluff, W.F., and Sharpless, N.E. (2013). Circular RNAs are abundant, conserved, and associated with ALU repeats. RNA *19*, 141–157.

Karreth, F.A., Reschke, M., Ruocco, A., Ng, C., Chapuy, B., Léopold, V., Sjoberg, M., Keane, T.M., Verma, A., Ala, U., et al. (2015). The BRAF pseudogene functions as a competitive endogenous RNA and induces lymphoma in vivo. Cell *161*, 319–332.

Krivtsov, A.V., and Armstrong, S.A. (2007). MLL translocations, histone modifications and leukaemia stem-cell development. Nat. Rev. Cancer *7*, 823–833.

Langmead, B., Trapnell, C., Pop, M., and Salzberg, S.L. (2009). Ultrafast and memory-efficient alignment of short DNA sequences to the human genome. Genome Biol. *10*, R25.

Lanotte, M., Martin-Thouvenin, V., Najman, S., Balerini, P., Valensi, F., and Berger, R. (1991). NB4, a maturation inducible cell line with t(15;17) marker isolated from a human acute promyelocytic leukemia (M3). Blood *77*, 1080–1086.

Lengfelder, E., Hofmann, W.K., and Nowak, D. (2012). Impact of arsenic trioxide in the treatment of acute promyelocytic leukemia. Leukemia *26*, 433–442.

Li, F., Zhang, L., Li, W., Deng, J., Zheng, J., An, M., Lu, J., and Zhou, Y. (2015a). Circular RNA ITCH has inhibitory effect on ESCC by suppressing the Wnt/β-catenin pathway. Oncotarget *6*, 6001–6013.

Li, P., Chen, S., Chen, H., Mo, X., Li, T., Shao, Y., Xiao, B., and Guo, J. (2015b). Using circular RNA as a novel type of biomarker in the screening of gastric cancer. Clin. Chim. Acta *444*, 132–136.

Li, Y., Zheng, Q., Bao, C., Li, S., Guo, W., Zhao, J., Chen, D., Gu, J., He, X., and Huang, S. (2015c). Circular RNA is enriched and stable in exosomes: a promising biomarker for cancer diagnosis. Cell Res. *25*, 981–984.

Li, Z., Huang, C., Bao, C., Chen, L., Lin, M., Wang, X., Zhong, G., Yu, B., Hu, W., Dai, L., et al. (2015d). Exon-intron circular RNAs regulate transcription in the nucleus. Nat. Struct. Mol. Biol. *22*, 256–264.

Liang, D., and Wilusz, J.E. (2014). Short intronic repeat sequences facilitate circular RNA production. Genes Dev. *28*, 2233–2247.

Löwenberg, B., Pabst, T., Vellenga, E., van Putten, W., Schouten, H.C., Graux, C., Ferrant, A., Sonneveld, P., Biemond, B.J., Gratwohl, A., et al.; Dutch-Belgian Cooperative Trial Group for Hemato-Oncology (HOVON) and Swiss Group for Clinical Cancer Research (SAKK) Collaborative Group (2011). Cytarabine dose for acute myeloid leukemia. N. Engl. J. Med. *364*, 1027–1036.

Lozzio, B.B., and Lozzio, C.B. (1979). Properties and usefulness of the original K-562 human myelogenous leukemia cell line. Leuk. Res. *3*, 363–370.

Martelli, M.P., Sozzi, G., Hernandez, L., Pettirossi, V., Navarro, A., Conte, D., Gasparini, P., Perrone, F., Modena, P., Pastorino, U., et al. (2009). EML4-ALK rearrangement in non-small cell lung cancer and non-tumor lung tissues. Am. J. Pathol. *174*, 661–670.

Memczak, S., Jens, M., Elefsinioti, A., Torti, F., Krueger, J., Rybak, A., Maier, L., Mackowiak, S.D., Gregersen, L.H., Munschauer, M., et al. (2013). Circular RNAs are a large class of animal RNAs with regulatory potency. Nature *495*, 333–338.

Meyerson, M., Gabriel, S., and Getz, G. (2010). Advances in understanding cancer genomes through second-generation sequencing. Nat. Rev. Genet. *11*, 685–696.

Qu, S., Yang, X., Li, X., Wang, J., Gao, Y., Shang, R., Sun, W., Dou, K., and Li, H. (2015). Circular RNA: A new star of noncoding RNAs. Cancer Lett. *365*, 141–148.

Rabbitts, T.H. (1994). Chromosomal translocations in human cancer. Nature *372*, 143–149.

Ryan, B.M., Robles, A.I., and Harris, C.C. (2010). Genetic variation in microRNA networks: the implications for cancer research. Nat. Rev. Cancer *10*, 389–402.

Salzman, J., Gawad, C., Wang, P.L., Lacayo, N., and Brown, P.O. (2012). Circular RNAs are the predominant transcript isoform from hundreds of human genes in diverse cell types. PLoS ONE *7*, e30733.

Salzman, J., Chen, R.E., Olsen, M.N., Wang, P.L., and Brown, P.O. (2013). Cell-type specific features of circular RNA expression. PLoS Genet. *9*, e1003777.

Smith, M.A., Morton, C.L., Phelps, D., Girtman, K., Neale, G., and Houghton, P.J. (2008). SK-NEP-1 and Rh1 are Ewing family tumor lines. Pediatr. Blood Cancer *50*, 703–706.

Somervaille, T.C., and Cleary, M.L. (2010). Grist for the MLL: how do MLL oncogenic fusion proteins generate leukemia stem cells? Int. J. Hematol. *91*, 735–741.

Tsuchiya, S., Yamabe, M., Yamaguchi, Y., Kobayashi, Y., Konno, T., and Tada, K. (1980). Establishment and characterization of a human acute monocytic leukemia cell line (THP-1). Int. J. Cancer *26*, 171–176.

Wang, Y., and Wang, Z. (2015). Efficient backsplicing produces translatable circular mRNAs. RNA *21*, 172–179.

You, X., Vlatkovic, I., Babic, A., Will, T., Epstein, I., Tushev, G., Akbalik, G., Wang, M., Glock, C., Quedenau, C., et al. (2015). Neural circular RNAs are derived from synaptic genes and regulated by development and plasticity. Nat. Neurosci. *18*, 603–610.

Zahreddine, H., and Borden, K.L. (2013). Mechanisms and insights into drug resistance in cancer. Front. Pharmacol. *4*, 28.

Zhang, X.O., Wang, H.B., Zhang, Y., Lu, X., Chen, L.L., and Yang, L. (2014). Complementary sequence-mediated exon circularization. Cell *159*, 134–147.

Zuber, J., Radtke, I., Pardee, T.S., Zhao, Z., Rappaport, A.R., Luo, W., McCurrach, M.E., Yang, M.M., Dolan, M.E., Kogan, S.C., et al. (2009). Mouse models of human AML accurately predict chemotherapy response. Genes Dev. *23*, 877–889.